Environ. Sci. Technol. **2004**, *38,* 6078−6084

NO and NO_2 Emission Ratios Measured from In-Use Commercial Aircraft during Taxi and Takeoff

SCOTT C. HERNDON,*,† JOANNE H. SHORTER,† MARK S. ZAHNISER,† DAVID D. NELSON, JR.,† JOHN JAYNE,† ROBERT C. BROWN,† RICHARD C. MIAKE-LYE,† IAN WAITZ,‡ PHILLIP SILVA,† THOMAS LANNI,§ KEN DEMERJIAN,|| AND CHARLES E. KOLB†

Aerodyne Research, Inc., 45 Manning Road, Billerica, Massachusetts 01821-3976, Department of Aeronautics and Astronautics, Massachusetts Institute of Technology, Cambridge Massachusetts 02139-4307, Department of Environmental Conservation, Albany, New York, 12233-3255, and Atmospheric Sciences Research Center and Department of Earth and Atmospheric Science, University at Albany, Albany, New York 12203

In August 2001, the Aerodyne Mobile Laboratory simultaneously measured NO, NO_2, and CO_2 within 350 m of a taxiway and 550 m of a runway at John F. Kennedy Airport. The meteorological conditions were such that taxi and takeoff plumes from individual aircraft were clearly resolved against background levels. NO and NO_2 concentrations were measured with 1 s time resolution using a dual tunable infrared laser differential absorption spectroscopy instrument, utilizing an astigmatic multipass Herriott cell. The CO_2 measurements were also obtained at 1 s time resolution using a commercial non-dispersive infrared absorption instrument. Plumes were measured from over 30 individual planes, ranging from turbo props to jumbo jets. NO_x emission indices were determined by examining the correlation between NO_x (NO + NO_2) and CO_2 during the plume measurements. Several aircraft tail numbers were unambiguously identified, allowing those specific airframe/engine combinations to be determined. The resulting NO_x emission indices from positively identified in-service operating airplanes are compared with the published International Civil Aviation Organization engine certification test database collected on new engines in certification test cells.

Introduction

The growing volume of commercial air traffic has raised concerns about the impact of aircraft exhaust emissions on atmospheric properties. Since commercial aircraft spend most of their flight time and expend much of their fuel in cruise mode in the upper troposphere and lower stratosphere, research over the past decade has focused on the current and projected impact of their exhaust emissions on regional to global scale ozone chemistry and the climate impact of light scattering and absorption of contrails and associated high altitude clouds. In 1999, an international assessment concluded that, while the impact of commercial aircraft on stratospheric ozone depletion was likely to be modest, the impact of ozone formation in the upper troposphere plus contrail and related cirrus cloud formation might lead to significant atmospheric warming over the first half of the 21st century (*1*, *2*).

Concerns about the impact of aviation emissions on the global atmosphere motivated advances to improve the measurement of gaseous and particulate aircraft engine emissions in both engine test cells that can simulate operation at altitude (*3*−*9*) and at cruise altitudes utilizing instrumentation on "chase" aircraft (*10*−*12*). Much of this effort has focused on quantifying NO_x (NO + NO_2) emissions because of their critical role in ozone chemistry, sulfur oxide emissions because of their role in triggering sulfate aerosol formation, and direct fine particulate emissions because of their role in contrail and cloud formation.

At the same time, attention has turned to the impact of aircraft emissions on local and regional air quality in the vicinity of airports (*13*,*34*,*35*). Here a primary focus is on NO_x emissions as initiators of photochemical smog and on fine particle emissions that can contribute to regional haze and directly impact human health (*14*). Unfortunately, much of the cruise operation emissions data gathered to assess the impact of aircraft emissions on the global atmosphere are of limited utility in assessing the airport emissions issue. Most of the airport emissions arise from gate, taxi, takeoff, and landing activities that are not well represented by cruise condition emissions. Only a few studies of aircraft emissions under normal airport operations have been published. The study by Popp et al. (*15*) measured NO/CO_2 emission ratios from in-use commercial aircraft at Heathrow Airport using open path IR and UV sensors developed for on-road motor vehicle emission measurements. Less directly relevant to normal operation emissions, Heland and Schäfer (*16*) and Schäfer et al. (*8*) analyzed Fourier transform infrared (FTIR) exhaust plume emission spectra taken for several cooperating commercial and military aircraft during run-up tests performed at German airports to yield CO_2, H_2O, CO, and NO exhaust mixing ratios used to compute CO and NO emission indices (EIs) as a function of engine power settings. Schäfer et al. (*17*) have also analyzed idle emissions from in-service airplanes and added NO_2 to the measurement suite. While the time a typical aircraft spends at idle is considerable, both the total fuel consumed and the NO_x emissions per fuel burned increase greatly during takeoff. Emissions need to be well characterized over these different modes of operation to fully assess their combined impact on air quality.

The present study has measured NO_x emissions for both idle and takeoff for in-service airplanes during routine operation at John F. Kennedy Airport. By sampling downwind of a taxiway and a runway, diluted exhaust plumes from individual airplanes were measured in both idle and takeoff modes, with "nudging" accelerations at above idle conditions also occasionally being observable. The data were collected in a totally noninterfering fashion, with no inconvenience to the observed airplane and no special considerations for the airport. By simultaneously measuring NO and NO_2, a better estimate of the NO_x EI can be computed, and some insight into the plume's chemical evolution can be gained.

* Corresponding author phone: (978)663-9500, ext 266; fax: (978)-663-4918; e-mail: herndon@aerodyne.com.
† Aerodyne Research, Inc.
‡ Massachusetts Institute of Technology.
§ Department of Environmental Conservation.
|| University at Albany.

10.1021/es049701c CCC: $27.50
Published on Web 10/13/2004

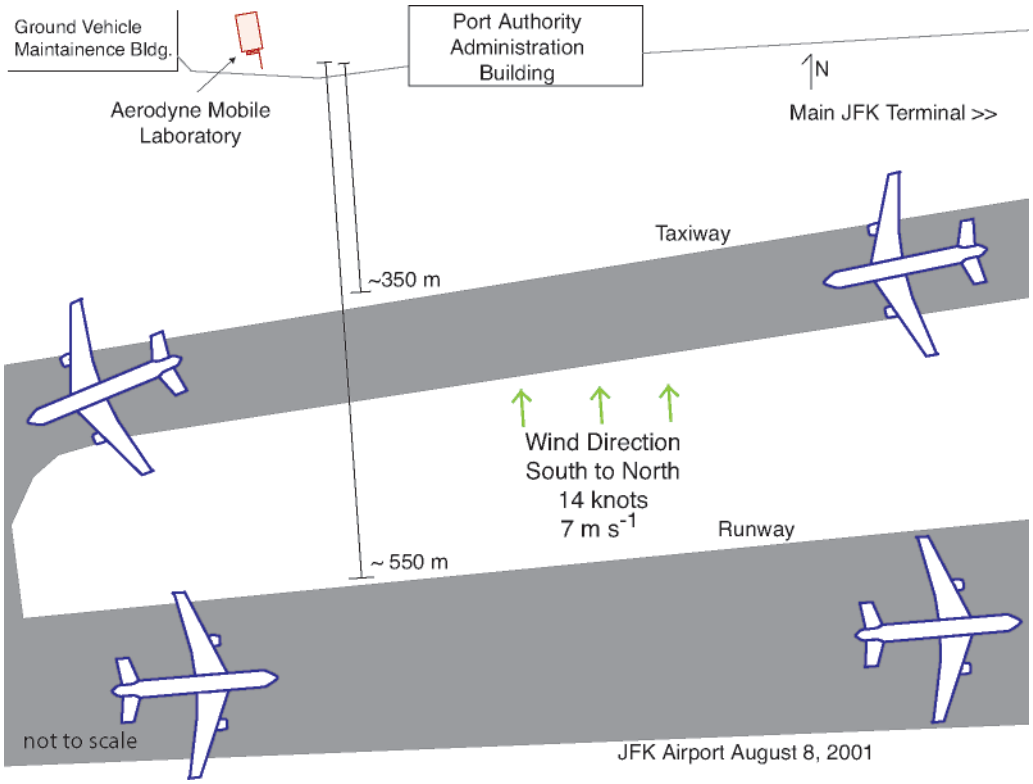

FIGURE 1. Approximate layout of the John F. Kennedy Airport site where these measurements were performed. The wind direction was a consistent 14 knots from the south throughout the measurement period. Aircraft moved across the wind field on the nearest taxiway, then turned, and took off on the runway. The mobile laboratory was positioned between the Port Authority Administration building and a maintenance building.

The Aerodyne Mobile Laboratory (*18*) was deployed in New York City as part of the $PM_{2.5}$ Technology Assessment and Characterization Study (PMTACS-NY). One component of the over all mission was the CNG/CRT Emission Perturbation Experiment (CEPEX) (*19*), which directed the Aerodyne Mobile Laboratory to "chase" curbside passenger buses along their routes in order to obtain real-world emission ratios over a representative drive cycle (*20*). Another goal of the CEPEX experiment was to attempt to measure an effective emission ratio for LaGuardia Airport. The prevailing weather during the scheduled time, however, did not afford the opportunity to sample downwind from La Guardia so we moved to John F. Kennedy Airport. Though other emission sources were observed (for example, ground support vehicles and helicopter takeoff), the focus of this work is on the in-use commercial aircraft emission ratios.

Experimental Section

On August 2, 2001, the Aerodyne Mobile Laboratory was positioned within 350 m of an in-use taxiway at John F. Kennedy Airport in New York City, with the cooperation of the Operations Director at the airport. The prevailing wind was a steady 7 m s^{-1} (14 knots) at a slight angle across a runway being used for takeoff and nearly normal to the taxiway accessing the end of this runway. A depiction of this layout is given in Figure 1. During takeoff, the wind carried exhaust plumes from the aircraft to the Aerodyne Mobile Laboratory when the aircraft had traveled approximately 300 m or the first tenth of the runway distance.

The Aerodyne Mobile Laboratory from which these measurements were conducted has been described in a previous publication (*18*), so only the specific instrumentation deployed on this mission will be discussed. The mobile laboratory was configured (*20*) with the gas phase and particulate instrumentation sharing a common sample inlet through the bulkhead of the truck located above the driver. A 1 in. o.d. stainless steel tube protruded forward at a height of ~2.4 m above the road level. The total flow at the inlet tip was measured to be 20 200 standard cm^3. Inside the truck, this flow was isokinetically split to provide sample to the various instruments. This paper focuses on the measurements of NO and NO_2 by Tunable Diode Laser Differential Absorption Spectroscopy (TILDAS) and of CO_2 using a commercial non-dispersive infrared absorption technique (Licor model 6262). The ability to take simultaneous measurements of other gaseous species and fine aerosol has been utilized in experiments measuring trucks and busses but was not fully exploited in the tests described here.

After the first isokinetic split, the TILDAS instrument and the Licor drew sample through 3.8 and 4.6 m lengths of $^1/_4$ in. PFA Teflon, respectively. The mass flows through the TILDAS and CO_2 analyzer were ~9000 and ~500 standard cm^3, and each flow was regulated by a critical pressure drop across an adjustable needle valve. In the TILDAS system, the needle valve is "upstream" from the instrument as the cell is operated at low pressure. The Licor instrument was operated at near ambient pressure, and its flow regulating needle valve was located "downstream" from the instrument. Lag times for CO_2 and NO were measured by making a "good to the second" note in the data stream by an operator inside the van at the moment an operator outside briefly opened and closed the cap on a sample of generator exhaust. Calculations of the lag time from the inlet to the two instruments using bulk flow velocity matched the measured lag times within 15% (3.8 and 4.8 s for the TILDAS and Licor, respectively).

The TILDAS technique has been described thoroughly elsewhere (*21*, *22*) and has been employed in several field measurement campaigns (*6*, *7*, *9*, *23*, *24*), but the specific instrument used for these measurements will be described.

IR light beams from two tunable lead-salt diode lasers (for NO and NO_2) were directed through an astigmatic multipass cell (*21*) and imaged onto separate detectors. The total number of passes for each beam through the cell was 174, for a total path length in the absorption cell of 153.5 m and a volume of 5 L. The laser frequency was swept over a narrow region (less than 1 cm^{-1}) at a repetition rate greater than 3 kHz with synchronous detection of the transmitted light. The resulting rotation−vibration transmission spectra were co-added for 1 s and fit using a Voigt line shape model (*25*, *26*) and line parameter data from the HITRAN database (*27*). For each of the diode lasers employed in these measurements, the laser line width is estimated to be less than 0.001 cm^{-1}. The pressure in the absorption cell was measured using a calibrated capacitance manometer, and for the measurements presented here, the pressure was 34−35.5 Torr. The temperature in the absorption cell was measured using a calibrated thermocouple. The optical table component of the TILDAS instrument was covered and heated to 31 °C to provide thermal stability. Temperatures of the gas in the absorption cell were within 0.5 °C of this temperature. Using bulk flow calculations, the response time of this instrument is estimated to be 0.92 s for 9 standard L min^{-1} at 35 Torr.

NO_2 was detected using an absorption feature at 1585.282 cm^{-1}. Of the species in the HITRAN database in this wavelength region, the next strongest absorber (CH_4) has nearby absorption lines which are 6 orders of magnitude weaker than the NO_2 lines used in these measurements. Therefore, the measurements of NO_2 by tunable diode laser spectroscopy are interference-free. Similarly, NO was detected using the cluster of lines at 1930.056 cm^{-1}, without any known interferences. As operated during these measurements, the 1 s root mean square (rms) precisions for NO_2 and NO were 190 and 550 ppt, respectively. The mode purity of the diode was verified by measuring NO or NO_2 in a reference cell along another optical path present in the instrument. The accuracy of the concentrations measured by TILDAS is largely determined by how well the line strengths are known. For the absorption lines used in the two instrument channels, the presently accepted band strengths for NO and NO_2 are known to within 6% and 4%, respectively (*28*).

The Licor (model 6262) non-dispersive IR absorption instrument detects CO_2 absorption in the 4.3 μm band. The precision in the 1 s Licor measurement was ~0.05 ppm rms, determined by sampling background that was apparently free from local combustion sources. The reproducibility of the CO_2 mixing ratio, estimated using an onboard calibration tank (600 ppm) and periodic measurements (2/week), is better than 0.8% (peak to peak). The manufacturer's quoted accuracy is ±0.5% under the conditions of instrument operation in the mobile laboratory. The measured response time of the Licor instrument to flooding the inlet tip with CO_2-free nitrogen gas results in an exponential decay with a time constant between 0.9 and 1.2 s.

In addition to the instruments, time-coded notes were recorded by the operators in the truck. A webcam automatically captured images of the upwind field of view every other second with a time code synchronized to the operator notes and the instrument data-logging. The NO, NO_2, and CO_2 mixing ratios were displayed in near real-time to the operators to facilitate proper positioning of the Aerodyne Mobile Laboratory.

Data Analysis. Let the concentration of a given species being emitted at the engine exit be represented by y_x and the ambient levels represented by y_a. Likewise, let the concentration of carbon dioxide (CO_2) be given by c_x and c_a (engine exit and ambient, respectively). When plumes are advected from taxiway or runway to the mobile laboratory, the sampled concentration will be represented by some combination of the emitted concentration and the ambient level depending on the dilution. Let f be defined as the volume fraction of exhaust plume for a given sampled volume in the measurement period (~1 s). If the subscript m refers to the measured concentration, it can be shown that

$$y_m = (1 - f)y_a + fy_x \quad (1)$$

If $f = 1$, this implies that pure exhaust is being measured, and when $f = 0$, strictly ambient levels are being sampled. We are interested measuring the emission ratio (ER) for species y defined in this context as

$$\mathrm{ER}(y) = \frac{y_x}{c_x} \quad (2)$$

Solving eq 1 for f, we obtain the following:

$$f = \frac{y_m - y_a}{y_x - y_a} \quad (3)$$

This expression will hold for the dilution of CO_2 as well, giving the main equation for the determination of ERs:

$$\frac{y_m - y_a}{y_x - y_a} = \frac{c_m - c_a}{c_x - c_a} \quad (4)$$

Equation 4 assumes that the response times for the measurement of species y and CO_2 are well matched. With the concentration of CO_2 in engine exit plume in excess of 2% (*29*) and ambient levels generally below 400 ppm, the following approximation is good to better than 2%:

$$c_x - c_a \cong c_x \quad (5)$$

Using the approximation eq 5 and either using the analogous approximation for y_m following eq 5 or using the knowledge that c_m/c_x is generally smaller than 0.05, eq 4 simplifies to the intuitive expression:

$$\mathrm{ER}(y)(c_m - c_a) = (y_m - y_a) \quad (6)$$

If the concentration y_m is plotted against c_m, a very simple diagnostic arises that resembles a locus of points around the ambient concentrations of y and CO_2 with rays extending toward higher concentrations of CO_2 when a plume is sampled. The slope of the correlation is indicative of the ER for species y under the conditions that emitted the partially sampled plume.

For the NO, NO_2, and CO_2 measurements presented in this work, the flow the response times of the instruments are well matched and the lag times well characterized. The measurements are continuous and the wind field steady. As air mixed with variable exhaust content advected to and past the sampling point, "plumes" were recognized by a concomitant rise in NO, NO_2, and CO_2. The duration of the aircraft plumes as they were blown to and past the sample inlet was between 18 and 32 s. Because the plumes are long relative to the 1 s response time of the instruments, the measured concentrations are used in eq 6 without any further averaging, convolution, or manipulation.

Emission Ratio and Emission Index. When the data acquired in this work is analyzed using eq 6, the quantity derived is an emission ratio with units of moles of NO_x per mole of CO_2. Generally, the International Civil Aviation Organization (ICAO) database and other industry measurements of NO_x use emission index (EI), in units of grams of NO_x (as NO_2) per kilogram of fuel. All NO_x EIs reported in this work are derived from the sum of the measured NO and NO_2 emission ratios and reported as grams of NO_2 per kilogram

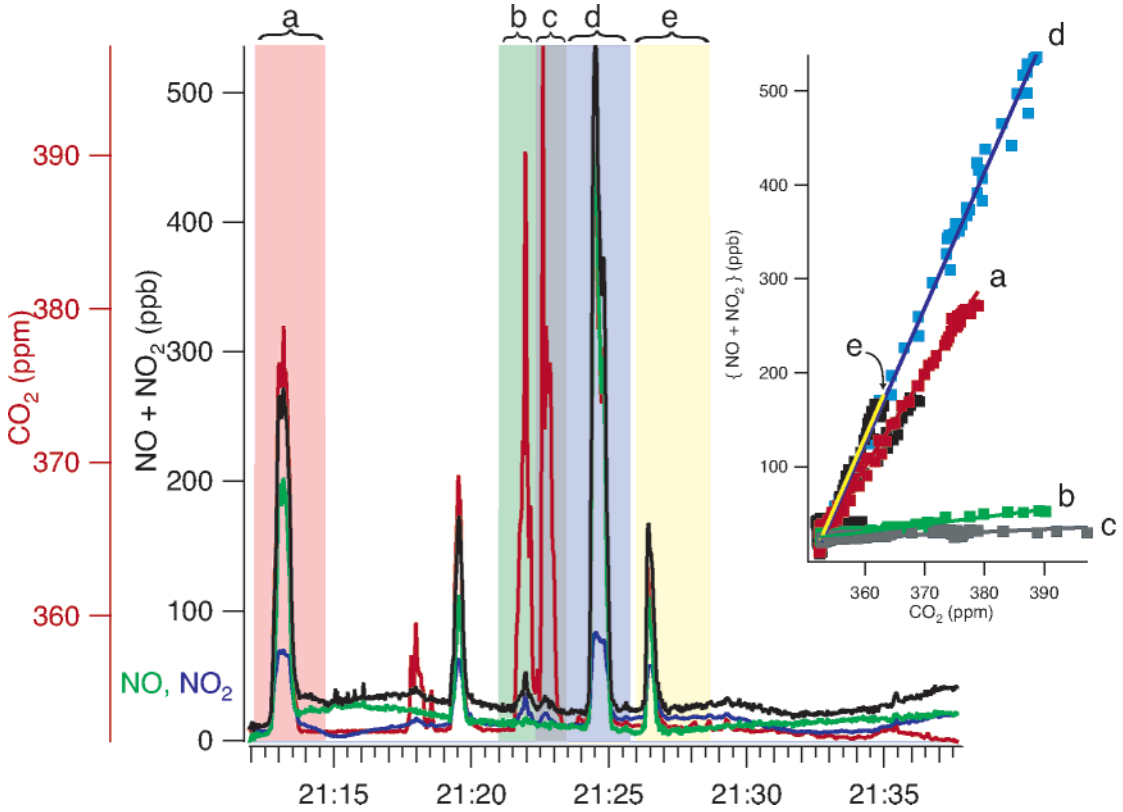

FIGURE 2. Temporal profile of takeoff and taxiway plumes arriving at the mobile laboratory. CO_2 is shown in red, NO_2 is in blue, NO is green, and the sum of NO and NO_2 (measured independently) is depicted as NO_x in black. Note the different scale for CO_2 and for the nitrogen oxide species. Pastel-shaded periods shown on the data vs time graph are shown with a letter corresponding to the lines in the inset graph. The inset graph lines show 1 Hz data for NO_x against CO_2 for different activities observed. Letters a, d, and e correspond to airplanes taking off; letters b and c represent airplanes taxiing.

of fuel. To convert the emission ratios measured in this work to EIs, a CO_2 EI is required. Spicer et al. (*29*) report that a CFM-56 jet engine at 7% idle emits roughly 97% of the fuel carbon as CO_2; with increasing throttle settings, this efficiency is increased to 99+%. For all conversions in this work, however, the value of the CO_2 EI is assumed to be 3160 g of CO_2 (kg of fuel)$^{-1}$, irrespective of throttle setting. This corresponds to 13.7% hydrogen content in the fuel.

Results

The Aerodyne Mobile Laboratory sampled downwind from the taxiway and runway as depicted in Figure 1 for two periods from about 7:00 pm to 9:30 pm in September 2001. All of the data presented is from this period. Fifteen minutes of data have been invalidated while a liquid nitrogen dewar, cooling the lasers and detectors, was replenished. An example of the measured data in time is shown along with the correlation plot in Figure 2. Review of the webcam images and time-coded notes allowed an accurate activity log to be constructed. The wind speed, distance from the taxiway and runway, and apparent delays based on the plume arrival times are consistent with the activity log (57−64 s for taxiway plumes and 87−102 s for runway plumes). For example, in Figure 2 the activity log indicates the plumes at 21:13, 21:19, 21:24, and 21:26 are all takeoff plumes while those at 21:18, 21:22, and 21:23 are plumes resulting from the aircraft rolling past on the taxiway. The principal reason it is important to have a firm understanding of the activity that resulted in the plume is hinted at in the inset of Figure 2, which shows the total NO_x (NO + NO_2) versus CO_2 for each of the 1 s measurements for the period shown by the time trace. The different emission ratios present in the plumes is a strong function of whether the aircraft was taxiing or operating near maximum throttle for takeoff. An intermediate activity was defined as "taxiway acceleration". This occurred when the number of aircraft waiting to takeoff on the taxiway approached 6. The line of aircraft would essentially be stationary, but then upon a takeoff, each of the aircraft would move forward.

The distribution of emission ratios determined during this 2 h sample period is shown in Figure 3. A clean taxi plume was actually most discernible when there was no taxiway "stop-and-go" activity. When a single aircraft moved past on the taxiway, the observed exhaust plume was what was deemed a taxi plume. When there was stop-and-go, there would be considerable nudging forward bit by bit—and this is what defined the intermediate condition, denoted taxiway acceleration in Figure 3. A takeoff plume was also easily discerned due to the very episodic nature and regularity with which the plume arrived. Because the sampled plumes originated fairly close to the beginning of the runway, the engines may not be completely equilibrated at full takeoff power. Also, the actual power condition chosen for takeoff may be dependent on the passenger and cargo loading on a particular airplane. Direct comparison with engine certification data may need qualification. On the other hand, the measurements do represent the emissions of NO_x under actual engine operation and demonstrate the potential to obtain such data in an operating airport without interfering with either the airplane or the airport itself.

Plume Evolution Model. In addition to measuring the total NO_x, the speciation between NO and NO_2 was also determined. It was observed that the ratio of NO to total NO_x was not uniform throughout the entire plume. This observation is consistent with the conversion of NO to NO_2 taking place via reaction with ozone.

A kinetic model was used to determine if ambient O_3 oxidation of NO to NO_2 in the plume is consistent with

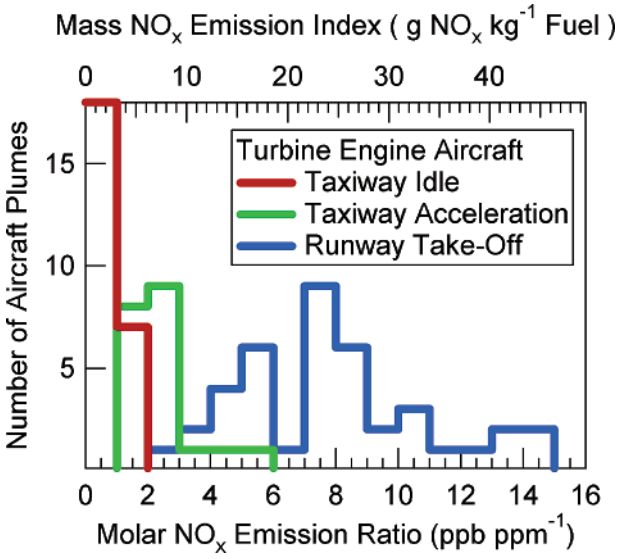

FIGURE 3. Frequency distribution of the measured emission ratios from in-use aircraft at John F. Kennedy Airport. The lower axis is the actual measured emission ratio while the upper axis assumes the engine conditions produced 3160 g of CO_2 (kg of fuel)$^{-1}$. Three different types of plumes are discerned: those due to takeoff are shown in blue (41 aircraft); the taxiway plumes representative of an idling engine are shown in red (25 aircraft); while intermediate plumes are shown in green (20 aircraft). See text for additional details on how the different types of plumes were determined.

measured NO_2/NO_x ratios. This model is a one-dimensional model for an evolving packet of aircraft engine exhaust gas that was developed based on a detailed microphysical model for gas-phase kinetics and aerosol particle dynamics in gas turbine engine exhaust plumes (*30*). This model was used to characterize the chemical evolution of engine emissions as they are carried toward the detector by a cross wind and proceeded in three steps.

First, the Standard Plume Flowfield (SPF) model (*31*) was used to characterize the evolution of engine emissions as a function of downstream distance from the engine exit plane. SPF is an axisymmetric parabolic Navier−Stokes flow code with embedded finite rate chemical kinetics. While it is not capable of treating wing−vortex interactions, it can simulate chemical changes in the exhaust gas from an aircraft engine with time (or downstream distance from the engine exit). This provides initial species conditions in the absence of any cross-wind interactions.

With cross-wind interactions, the flow field is exceedingly more complicated and was not rigorously treated. Rather, for the second stage of the calculation, it was assumed that an initial state could be defined in which a parcel of engine exhaust gas (i.e., gas dynamic properties and species mixing ratio from SPF) at some downstream distance from the engine exit was instantaneously diluted with ambient air. The speciation in this diluted parcel of exhaust gas provides the initial conditions for the one-dimension model calculation.

For the third and final step in the calculation, this diluted engine exhaust gas parcel was then allowed to evolve due to advection toward the detector. Further air entrainment was treated using a simple one-dimensional mixing profile with finite-rate NO oxidation chemistry included.

For the procedure described above, the initial mixing and one-dimensional mixing profile were adjustable model parameters that collectively are constrained by the engine emission level of CO_2 at the engine exit and the measured level of CO_2 at the detector. Thus the overall dilution was specified while the dilution time history was adjusted by varying the initial mixing state and one-dimensional mixing profile. The concentration of O_3 in the diluent air was assumed to be 30 ppb. Monitoring stations at Queen's College and the Queensboro Community College show the ozone concentration falling from 44 to 23 ppb over the course of these experiments (*32*).

Figure 4 shows the calculated NO_2/NO_x ratio based on assuming a fast and slow dilution rate at selected times between 50 and 100 s. Initial engine exit emission levels were selected to be representative of emissions for a B757. The model calculations yield NO_2/NO_x ratio ranging between 32 and 36%. For shorter times, a faster mixing produces a little higher NO to NO_2 conversion. However, the differences in NO oxidation due to differences in dilution rates are relatively small for time scales on the order of several tens of seconds. For the present case, after approximately 95 s, details of the dilution history have been washed out. The modeled conversion fraction is sensitive to the concentration of O_3; a 10% change in O_3 (about 30 ppbv) results in a 4% change in the fraction of NO_2/NO_x.

The measured NO_2/NO_x ratios range between 28 and 35%. These calculation results are consistent with measured NO_2/NO_x ratios and suggest that the measured ratios reflect NO to NO_2 conversion due O_3 oxidation in parcels of engine exhaust gas as they advect toward the detector.

Discussion

For three airplane measurements, the specific airplane model and the airplane/engine combination were identified. Due to limitations of data extraction from the webcam video and due to difficulties in identifying international traffic, the other airplanes in our data set could not be identified post facto. In future studies, however, tail numbers could be specifically recorded during measurement to aid in this identification process. In the current study, the identification of the three engines allowed a comparison of the measured EIs with those determined during the certification tests for those types of engines, which are recorded in the ICAO database. These comparisons are made in Table 1 for takeoff and idle. The top section of the table shows the results, while the bottom section of the table provides additional information on the engine. To discuss the comparison between these measurements and the ICAO certification values, it is important to consider the expected variability and experimental uncertainty. A review of the expected engine-to-engine variability (∼7%) and modeled estimate of the aging effects (−1 to 4%) on NO_x emission ratio (*33*) suggests that the ICAO certification values in Table 1, when compared with a specific measurement, should be good to ∼10%. The individual 2σ precision uncertainties are listed with each measurement in Table 1, but generally for "takeoff" the experimental noise is <7%. The absolute accuracy of the instrumentation and estimates of other sources of error results in a systematic uncertainty of ∼8%. An additional uncertainty present in the reported NO_x EI computed from the measured emission ratios involves the CO_2 EI. In this work, an EI of 3160 g of CO_2 (kg of fuel)$^{-1}$ has been assumed for all throttle settings. On the basis of previous measurements (*29*) of CO_2 as a function of fuel flow and engine operating condition and the variability of field observations of CO EIs (*17*), the assumption of a constant CO_2 EI introduces an additional 4% error in the computed NO_x EI. Given the expected variability and measurement uncertainty, the agreement between the ICAO database and these measurements is very good. To improve future studies, other EIs such as those for carbon monoxide or total hydrocarbons could aid in determining the appropriate throttle setting. Measurements at various locations along the runway could address uncertainties in the throttle settings used during takeoff.

The taxiway or idle plume comparison is also made in Table 1. Each of the taxiway plumes is lower than the ICAO

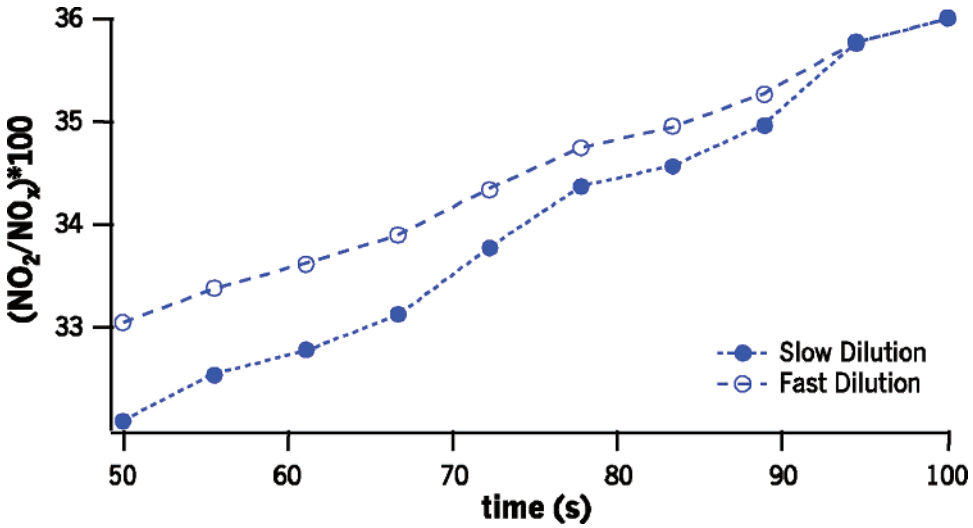

FIGURE 4. Calculated NO_2/NO_x ratio for two engine exit dilution cases as a function of time, using the Standard Plume Flowfield model (see text for additional details). A B757 was chosen for the engine exit emissions data in these simulations.

TABLE 1. Comparison of Measured Emission Indices to ICAO Reference Values

aircraft[a]	state	ICAO g of NO_x (kg of fuel)$^{-1}$	measd[b,c] g of NO_x (kg of fuel)$^{-1}$ (as NO_2)
A	taxiway[d]	3.15	2.9 ± 0.4
	takeoff[e]	17.1	19 ± 1.1
B	taxiway	3.6	1.6 ± 0.2
	takeoff	27	29 ± 2
C	taxiway	4.7	3.4 ± 1
	takeoff	26.5	25.2 ± 0.9

aircraft[a]	engine mfg	airframe mfg	aircraft
A	Pratt & Whitney JT8D-7B	Douglas	DC-9-30 stage 3
B	Pratt & Whitney JT8D-219	Boeing	DC-9-83
C	International Aero.	Airbus Industrie	A320-200

[a] For these three measurements (A–C), the specific airplane model and the airplane/engine combinations were identified (*34*) via their tail number. [b] Conversion of measured emission ratio NO_x/CO_2 (mmol mol^{-1}) assumes a constant 3160 g of CO_2 (kg of fuel)$^{-1}$ for each aircraft. [c] Error limits determined from 2σ in the precision of the fit. [d] ICAO Engine Exhaust Emissions Data Bank data defines "idle" to be 7% throttle (see text for description of taxiway idle vs taxiway acceleration). [e] ICAO Engine Exhaust Emissions Data Bank data taken for "takeoff" or 100% power.

certification value. It is likely that the engine condition for the sampled plumes was less than the 7% throttle specified by the ICAO certification process for "idle".

The NO_x emission ratios determined in this work agree with the NO EIs measured by Popp et al. (*15*) at Heathrow Airport. Though the distribution of the results of the individual aircraft is not shown in their paper, the overall summary cites a breakdown of the measured aircraft into three categories; EI less than 5 g kg^{-1}, between 5 and 15 g kg^{-1}, and greater than 15 g kg^{-1}. The authors note that aircraft measured in this last category were observed to be increasing power as they turned from taxiway to runway for immediate takeoff. Their results have a character similar to the data in Figure 3. The wind information and video record present in this work allows facile identification of the aircraft and activity producing the observed plumes.

Conclusion

Emissions from airplanes are assessed in environmental impact studies of airports, and EIs are used in conjunction with models of airport operations to estimate the contribution airplanes make to the local emissions inventory. One uncertainty in performing these studies is the accuracy of the EIs used for the airplanes represented in the airport operations. The emissions measured during certification of new airplane engines at four nominal power conditions in an engine test cell, which are normally used in such environmental assessments, may not be representative of emissions during routine operation of in-service airplanes. The measurement approach demonstrated in the present study shows that an intercomparison between certification data and in-service emissions can be made with little or no interference with airport operations. Also, for the small sample of three airplane/engines analyzed here, the comparison between ICAO and in-service engines is very good. A larger sampling of engine types and more sampling points within the airport would allow a much broader and more detailed comparison to be carried out to better evaluate the applicability of ICAO data to in-service airplanes.

These measurements have demonstrated that it is possible to measure real world emission ratios from in-use commercial aircraft with no disruption to service and modest cooperation from airport officials. For the three aircraft that were unambiguously identified, comparison of the measured emission ratio to the ICAO EI agrees within the expected engine-to-engine variability, aging effects, and experimental uncertainty for three somewhat different engine types. The agreement is a promising first result, but additional measurements would be required to examine the potential differences between emission ratio during engine certification and in-use conditions. This technique could potentially get simultaneous data on the EI during different operating conditions and the averaged duty cycle for an airplane departure: idle time, taxiway time, and takeoff duration, for example. Experiments designed with this technique could be used to obtain results that may aid modeling efforts to assess airport emissions in an urban air quality context. Although this work has focused on the NO_x emission ratio measurements, this general measurement approach would allow additional gaseous species and particulate to be determined using other measurement technologies.

Acknowledgments

The Port Authority of New York and New Jersey, specifically LaGuardia and John F. Kennedy International Airport Operations Staff; '99', '97', and '93' Federal Aviation Administration for aircraft tail number data; Brian Kim and

Gregg Fleming of Volpe National Transportation Systems Center for identification of the specific aircraft types from the video record EPA Supersite Programs: PMTACS-NY and CEPEX.

Literature Cited

(1) IPCC, Ed. *Aviation and the Global Atmosphere, Intergovernmental Panel on Global Change*; Cambridge University Press: Cambridge, 1999.

(2) Miake-Lye, R. C.; Waitz, I.; Fahey, D.; Wesoky, H.; Wey, C. Aviation and the changing climate. *Aerospace Am.* **2000**, 35−39.

(3) Böckle, S.; Einecke, S.; Hildenbrand, F.; Orlemann, C.; Schulz, C.; Wolfrum, J.; Sick, V. Laser-spectroscopic investigation of OH-radical concentrations in the exhaust plane of jet engines. *Geophys Res. Lett.* **1999**, *26*, 1849−1852.

(4) Wiesen, P.; Kleffmann, J.; Kurtenbach, R.; Becker, K. H. Nitrous oxide and methane emissions from aero engines. *Geophys. Res. Lett.* **1994**, *21*, 2027−2030.

(5) Wiesen, P., Kleffmann, J.; Kurtenbach, R.; Becker, K. H. Emission of nitrous oxide and methane from aero engines: monitoring by tunable diode laser spectroscopy. *Infrared Phys. Technol.* **1996**, *37*, 75−81.

(6) Howard, R. P.; et al. *Experimental Characterization of Gas Turbine Emissions at Simulated Flight Altitude Conditions*; U.S. Air Force Arnold Engineering Development Center: 1996; AEDC-TR-96-3.

(7) Wey, C. C.; Wey, C.; Dicki, D. J.; Loos, K. H.; Noss, D. E.; Hagen, D. E.; Whitefield, P. D.; Trueblood, M. B.; Wilson, M. E.; Olson, D.; Ballenthin, J. O.; Miller, T. M.; Wiggiano, A. A.; Wormhoudt, J.; Berkoff, T.; Miake-Lye R. C. *Engine Gaseous, Aerosol Precursor and Particulate at Simulated Flight Altitude Conditions*; National Aeronautics and Space Administration: 1998.

(8) Schäfer, K.; Heland, J.; Lister, D. H.; Wilson, C. W.; Howes, R. J.; Falk, R. S.; Lindermeir, E.; Birk, M.; Wagner, G.; Haschberger, P.; Bernard, M.; Legras, O.; Wiesen, P.; Kurtenbach, R.; Brockmann, K. J.; Kriesche, V.; Hilton, M.; Bishop, G.; Clarke, R.; Workman, J.; Caola, M.; Geatches, R.; Burrows, R.; Black, J. D.; Hervé, P.; Vally, J. Nonintrusive optical measurements of aircraft engine exhaust emissions and comparison with standard intrusive techniques. *Appl. Opt.* **2000**, *39*, 441−455.

(9) Whitefield, P. D.; Hagen, D. E.; Wormhoudt, J. C.; Miake-Lye, R. C.; Wilson, C.; Brundish, K.; Waitz, I.; Lukachko, S.; Yam C. K. *NASA/QinetiQ Collaborative Program—Final Report*; National Aeronautics and Space Administration: 2002.

(10) Fahey, D. W.; Keim, E. R.; Boering, K. A.; Brock, C. A.; Wilson, J. C.; Jonsson, H. H.; Anthony, S.; Hanisco, T. F.; Wennberg, P. O.; Miake-Lye, R. C.; Salawitch, R. J.; Louisnard, N.; Woodbridge, E. L.; Gao, R. S.; Donnelly, S. G.; Wamsley, R. C.; Del Negro, L. A.; Solomon, S.; Daube, B. C.; Wofsy, S. C.; Webster, C. R.; May, R. D.; Kelly, K. K.; Loewenstein, M.; Podolske, J. R.; Chan, K. R. Emission measurements of the Concorde Supersonic aircraft in the lower stratosphere. *Science* **1995**, *270*, 70−74.

(11) Schulte, P.; Schlager, H.; Ziereis, H.; Schumann, U.; Baughcum, S. L.; Deidewig, F., NOx emission indices of subsonic long-range jeft aircraft at cruise altitude: In situ measurements and predictions. *J. Geophys. Res.* **1997**, *102*, 21431−21442.

(12) Schumann, U.; Arnold, F.; Busen, R.; Curtius, J.; Kärcher, B.; Kiendler, A.; Petzold, A.; Schlager, H.; Schröder, F.; Wohlfrom, K.-H. Influence of fuel sulfur on the composition of aircraft exhaust plumes: The experiments SULFUR 1−7. *J. Geophys. Res.* **2002**, *107*.

(13) Stedman, J. R.; Vincent, K. J.; Campbell, G. W.; Goodwin, J. W. L.; Downing, C. E. H. New high resolution maps of estimated background ambient NOx and NO2 concentrations in the UK. *Atmos. Environ.* **1997**, *31*, 3591−3602.

(14) Stedman, J. R.; Linehan, E.; King, K. *Quantification of the Health Effects of Air Pollution in the UK for the Review of the National Air Quality Strategy*; AEAT-4715; 1999; http://www.aeat.co.uk/netcen/airqual/reports/health/health2.pdf.

(15) Popp, P. J.; Bishop, G. A.; Stedman, D. H. Method for commercial aircraft nitric oxide emission measurements. *Environ. Sci. Technol.* **1999**, *33*, 1542−1544.

(16) Heland, J.; Schäfer, K. Determination of major combustion products in aircraft exhausts by FTIR emission spectroscopy. *Atmos. Environ.* **1998**, *32*, 3067−3072.

(17) Schäfer, K.; Jahn, C.; Sturm, P.; Lechner, B.; Bacher, M. Aircraft emission measurements by remote sensing methodologies at airports. *Atmos. Environ.* **2003**, *37*, 5261−5271.

(18) Kolb, C. E.; Herndon, S. C.; McManus, J. B.; Shorter, J. H.; Zahniser, M. S.; Nelson, D. D.; Jayne, J. T.; Canagaratna, M. R.; Worsnop, D. R., Mobile laboratory with rapid response instruments for real-time measurements of urban and regional trace gas and particulate distributions and emission source characteristics. *Environ. Sci. Technol.* **2004**, *21*, 5694−5703.

(19) Canagaratna, M. R.; Jayne, J. T.; Ghertner, A.; Herndon, S. C.; Shi, Q.; Jimenez, J. L.; Silva, P.; Williams, P.; Lanni, T.; Drewnick, F.; Demerjian, K. L.; Kolb, C. E.; Worsnop, D. R. Chase studies of particulate emissions from in-use New York City vehicles. *Aerosol Sci. Technol.* **2004**, *38*, 555−573.

(20) McManus, J. B.; Kebabian, P. L.; Zahniser, M. S. Astigmatic mirror multiple pass absorption cells for long pathlength spectroscopy. *Appl. Opt.* **1995**, *34*, 3336.

(21) Zahniser, M. S.; Nelson, D. D. J.; Kolb, C. E. In *Applied Combustion Diagnostics*; Kohse-Höinghaus, K., Jeffries, J. B., Eds.; Taylor & Francis: New York, 2002.

(22) Zahniser, M. S.; Nelson, D. D.; McManus, J. B.; Kebabian, P. L. Measurement of trace gas fluxes using tunable diode laser spectroscopy. *Philos. Trans. R. Soc. London A* **1995**, *351*, 357−369.

(23) Horii, C. V.; Zahniser, M. S.; Nelson, D. D.; McManus, J. B.; Wofsy, S. C. Nitric acid and nitrogen dioxide flux measurements: A new application of tunable diode laser absorption spectroscopy. Application of tunable diode and other infrared sources for atmospheric studies and industrial process monitoring; *SPIE Proc.* **1999**, *3758*, 152−161.

(24) Armstrong, B. H. Spectrum line profiles: The Voigt function. *J. Quant. Spectrosc. Radiat. Transfer* **1967**, *7*, 61−88.

(25) Humlicek, *J. Quant. Spectrosc. Radiat. Transfer* **1979**, *21*, 309−313.

(26) Rothman, L. S.; Rinsland, C. P.; Goldman, A.; Massie, S. T.; Edwards, D. P.; Flaud, J.-M.; Perrin, A.; Camy-Peyret, C.; Dana, V.; Mandin, J.-Y.; Schroeder, J.; McCann, A.; Gamache, R. R.; Wattson, R. B.; Yoshino, K.; Chance, K. V.; Jucks, K. W.; Brown, L. R.; Mentchinov, V.; Varanasi, P. The Hitran molecular spectroscopic database and Hawks (HItran Atmospheric Workstation): 1996 Edition. *J. Quant. Spectrosc. Radiat. Transfer* **1998**, *60*, 665−710.

(27) Smith, M. A. H.; Rinsland, C. P.; Fridovich, B.; Rao, K. N. In *Molecular Spectroscopy: Modern Research*; Academic Press: New York, 1985; Chapter 3.

(28) Spicer, C. W.; Holdren, M. W.; Riggin, R. M.; Lyon, T. F. Chemical composition anf photochemical reactivity of exhaust from aircraft turbine engines. *Ann. Geophys.* **1994**, *12*, 944−955.

(29) Brown, R. C.; Miake-Lye, R. C.; Anderson, M.; Kolb, C. E.; Resch, T. J. Aerosol dynamics in near-field aircraft plumes. *J. Geophys. Res.* **1996**, *101*, 22,939−22,953.

(30) Dash, S. M.; Pergament, H. S.; Wolf, D. E.; Sinha, N.; Taylor, M. W.; Vaughn, M. E. *The JANNAF Standard Plume Flowfield Code Version II* (*SPF-II*); U.S. Army Missle Command: Huntsville, AL, 1990.

(31) Demerjian, K. L. Data from the monitoring stations at Queensboro Community College and Queen's College show ozone trending from 46 to 20 and from 42 to 27 ppb, resepectively, while these measurements were conducted.

(32) Lukachko, S. P.; Waitz, I. A. Effects of engine aging on aircraft NOx emissions. *International Gas Turbine & Aeroengine Congress & Exhibition*; Orlando, FL, 1997; 97-GT-386; pp 1−15.

(33) Associates, B. *Back Fleet Database v4.0*; Back Aviation Solutions: New Haven, CT, 2001.

(34) Underwood, B. Y.; Brightwell, S. M.; Peirce, M. J.; Walker, C. T. *Air quality at UK Regional Airport in 2005 and 2010*, AEAT/ENV/0452 Issue 2 2001; http://www.airquality.co.uk/archive/reports/cat07/aeat-env-r-0453.pdf, 42.

(35) Pison, I.; Menut, L. Quantification of the impact of aircraft traffic emissions on tropospheric ozone over Paris area *Atmos. Environ.* **2004**, *38*, 971−983.

Received for review February 25, 2004. Revised manuscript received August 5, 2004. Accepted August 24, 2004.

ES049701C